The porosity in a fluidized bed heat transfer model

G. VISSER and M. VALK

Department of Thermal Engineering, University of Twente, P.O. Box 217, 7500 AE Enschede,
The Netherlands

Abstract—A mathematical model of heat transfer between a fluidized bed and an immersed surface and a model of gas flow and porosity, both recently published, were combined and further modified in the area of low velocities where the particle convective component of heat transfer is low or neglectable. Experimental work consisted of measurements of both porosity and heat transfer in a cold fluidized bed of sand. Five samples of sand, each having a narrow size range, were investigated; the mean particle diameter varied from 0.43 to 1.55 mm. Also two mixtures of these samples, which yielded a wide particle size distribution, were tested. Experimental results showed good agreement with model predictions, for both porosity and heat transfer.

INTRODUCTION

AN IMPORTANT property of fluidized beds applied in various chemical and physical processes is the high rate of heat transfer between the bed and the immersed surfaces. However, an accurate prediction of the heat transfer coefficient, necessary for a reliable design of fluidized bed equipment, is still difficult to obtain. During the past forty years, many models and correlations have been developed, but generally these are reliable in only a restricted area of operation. This is caused by the complexity of fluidized bed heat transfer and hydrodynamics with their many variables.

Heat transfer from a fluidized bed to a surface (or vice versa) consists of a particle convective, a gas convective and a radiative part. In most practical situations, a combination of two or three parts has to be considered, while previous literature only treats one part: either small particles whose primary heat transfer process is by particle convection, or large particles for which gas convective heat transfer is the most important mechanism.

Recently, Borodulya *et al.* [1] developed their two-zone model, based partly on theory and partly on experiments. This model provides a reliable prediction of the heat transfer coefficient over a wide range of pressures, temperatures and particle diameters. Dependence on fluidizing velocity, however, is not correctly taken into account, because the model neglects the decrease of particle convective heat transfer at velocities less than U_{opt} and the total absence of particle convection when the gas velocity is less than U_{mf}. At these velocities the bed is not fluidized, which implies that no replenishment of particles at the heat transfer surface takes place. Thus there is no temperature difference between bed and surface which is elementary for particle convection. Gas convective heat transfer is not affected by particle motion.

An important hydrodynamic variable in the model is the porosity or voidage of the bed material, because this variable determines the amount of gas convective relative to particle convective heat transfer. The original relations proposed in the model [2] to predict the porosity are partly based on the two-phase theory of fluidization, whose reliability in the case of large particles is not proven. For an accurate prediction of porosity a complete analysis of gas flow, solids motion and bed geometry is needed. Glicksman *et al.* [3] developed a model which applies to beds both with and without internals such as cooling pipe arrays.

In this investigation the porosity model of Glicksman and the heat transfer model of Borodulya were combined, and a modification was made to improve model predictions in the area of low velocities (from 0 to U_{opt}).

THEORY

Borodulya *et al.* [2] model the heat transfer coefficient as an effective conductivity divided by an effective conduction path length. The result is fitted with their own experimental results and with literature data. Their correlation for ambient temperature and pressure is

$$Nu = 7.2(1-\varepsilon)^{2/3} + 0.044 Re\ Pr(1-\varepsilon)^{2/3}/\varepsilon. \quad (1)$$

The first term represents the particle convective part, the second term the gas convective part of heat transfer. Later, Borodulya *et al.* [1] modified this formula so that it correctly describes the influence of particle diameter on heat transfer for small particles. This is done by introducing the Archimedes number into equation (1). After fitting with experimental results from the literature, the following formula results:

$$Nu = 2.62 Ar^{0.1}(1-\varepsilon)^{2/3} + 0.033 Re\ Pr(1-\varepsilon)^{2/3}/\varepsilon. \quad (2)$$

NOMENCLATURE

Ar Archimedes number, $gd_p^3\rho_f(\rho_p-\rho_f)/\mu_f^2$

c specific heat at constant pressure
[J kg^{-1} K^{-1}]

d diameter [m]

Fr modified Froude number, $(U-U_{mf})^2/gH_{mf}$

g gravitational acceleration [m s^{-2}]

H bed height [m]

h external heat transfer coefficient
[W m^{-2} K^{-1}]

K through-flow coefficient

N_0 number of orifices per m^2 in a distributor plate

Nu Nusselt number, hd_p/λ_f

Pr Prandtl number, $c_f\mu_f/\lambda_f$

p pressure [N m^{-2}]

Δp pressure difference [N m^{-2}]

Re Reynolds number, $Ud_p\rho_f/\mu_f$

U superficial gas velocity [m s^{-1}]

w weight fraction

z axial coordinate [m].

Greek symbols

δ bubble fraction

ε porosity

λ thermal conductivity [W m^{-1} K^{-1}]

μ dynamic viscosity [kg m^{-1} s^{-1}]

ρ density [kg m^{-3}].

Subscripts

B   bed

b   bubble

f   gas

i ith fraction

mf   minimum fluidization

opt   optimum

o   entrance

p   particles.

Formula (2) can be used when $0.1 < d_p < 4.0$ mm. Other correlations are developed for higher temperatures and pressures [1].

One objection against these formulas is that the particle convective term (thus the first term in both formulas) has a fixed minimum value when gas velocity drops down to zero (because of the minimum value for ε). In practice, however, particle convective heat transfer can be neglected at velocities below U_{mf} and is only small when $U_{mf} < U < U_{opt}$ because particles at the surface are stationary or seldom refreshed. To adapt the model to this phenomenon, a multiplication factor f was introduced, which provides a zero particle convection term at velocities below U_{mf} and a smooth increase between U_{mf} and U_{opt}

$$U < U_{mf}: \quad f = 0 \tag{3}$$

$$U_{mf} < U < U_{opt}: \quad f = \left(\frac{U-U_{mf}}{U_{opt}-U_{mf}}\right)^C \tag{4}$$

with C being a constant, and

$$U > U_{opt}: \quad f = 1. \tag{5}$$

A value of $C = 0.3$ proved to give the best results. Factor f is inserted in relation (2)

$$Nu = 2.62f\,Ar^{0.1}(1-\varepsilon)^{2/3}+0.033Re\,Pr(1-\varepsilon)^{2/3}/\varepsilon. \tag{6}$$

From equations (1), (2) and (6) it is clear that the porosity is an important parameter in the heat transfer process. The simple relationships to predict porosity, originally advised in the model [2], are

$$\varepsilon = 1-(1-\varepsilon_{mf})/(1+0.7(H_{mf}/d_B)^{1/2}Fr^{1/3}) \tag{7}$$

$$\varepsilon = \varepsilon_{mf}+1.56(Re-Re_{mf})(1-\varepsilon_{mf})/Ar^{1/2}. \tag{8}$$

This porosity model yields results which are too high at velocities beyond U_{opt}. A better model was recently described by Glicksman et al. [3]. It is based on a first-principles theory of gas flow. The model consists of five equations for use with different geometries, with and without pipes in the bed. We used the equations without pipes. These equations have to be solved simultaneously

$$K = \exp\left[\delta\left(1.4+\frac{7.6}{H/d_b}\right)\right]_{z=H} \tag{9}$$

$$U = KU_{mf}+\delta(U-U_{mf}+0.71\sqrt{(gd_b)}) \tag{10}$$

$$d_{bo} = \max\left\{\left[\frac{1.3}{g^{0.2}}\left(\frac{U-KU_{mf}}{N_0}\right)^{0.4}\right],\right.$$
$$\left.\left[3.69\frac{(U-KU_{mf})^2}{g}\right]\right\} \tag{11}$$

$$d_b =$$
$$\left[(d_{bo})^{10/7}+\frac{2.6z(U/U_{mf}-K)(U-U_{mf})^{6/7}}{(U/U_{mf}-1)g^{3/7}}\right]^{7/10} \tag{12}$$

$$H = H_{mf}/(1-\delta). \tag{13}$$

For other configurations we refer to ref. [3].

EXPERIMENTS

The experiments were executed in a cold fluidized bed, the internal diameter of which was 290 mm. With all experiments, the bed height at minimum fluidization was 300 mm. The bed was made of Plexiglas, and was mounted on a steel windbox. The distributor consisted of two perforated metal sheets and a felt
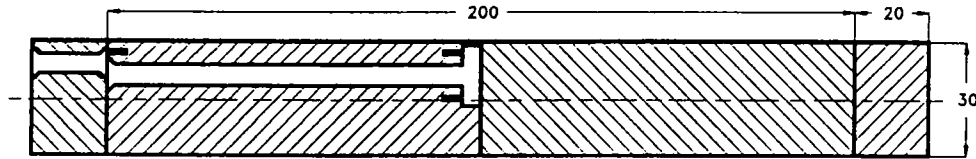
FIG. 1. Heat transfer probe.

cloth pressed in between, necessary to obtain a sufficient pressure drop over the distributor. Pressure transducers which could be inserted in the bed up to 150 mm from the wall, were mounted at distances of 50, 150, 250 and 350 mm above the distributor. The fluidizing air was supplied by a centrifugal blower, the maximum fluidizing velocity that could be obtained was 1.5 m s^{-1}. The mass flow of this air was measured. To measure the heat transfer coefficient from an immersed surface to the fluidized bed, we used a copper cylinder (Fig. 1), length 200 and diameter 30 mm. Both ends were insulated with Teflon cylinders, length 20 mm. Two copper–constantan thermocouples were used to measure the cylinder temperature. The cylinder was heated in an oven before being inserted in the bed. A temperature–time curve was registered during the period when the temperature difference between the cylinder and the bed sank from 70 to 41°C. The mean bed temperature was 35°C. For calculating Nu, a heat balance was used. We determined bed porosity by measuring pressure differences between probes at different heights in the bed. These differences are related to porosity by $\Delta p/\Delta p_{mf} = (1 - \varepsilon)/(1 - \varepsilon_{n.f})$ [4].

Sand sizes

The five samples of sand that were tested, had mean particle diameters of 0.43, 0.61, 0.86, 1.20, and 1.55 mm, respectively, and a narrow particle size distribution. Mixture 1 consisted of samples 1 and 3, in relative amounts so that the mean particle diameter according to

$$d_p = 1/\Sigma(w_i/d_{pi}) \qquad (14)$$

was 0.61 mm. In the same way mixture 2 consisted of samples 3 and 5, and had a mean particle diameter of 1.20 mm.

RESULTS AND DISCUSSION

For all sand samples and mixtures, we measured the porosity and heat transfer coefficient as a function of fluidizing velocity, which ranged from U_{mf} to 1.5 m s^{-1} in steps of approximately 0.1 m s^{-1}.

The experimental values of porosity were compared with the values calculated with relations (7) and (8) (Fig. 2). The standard deviation over all values, of the experimental relative to the calculated values is 0.046. The same experimental values are compared to the results of the calculations performed with the porosity model represented by equations (9)–(13) (Fig. 3).
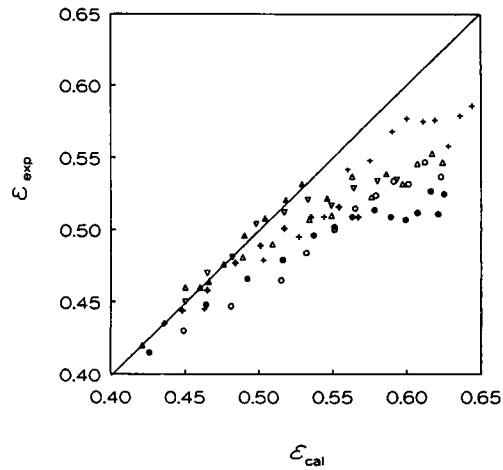

FIG. 2. Comparison between experimental results (samples 1–5 and mixtures 1, 2) and model calculations [equations (7) and (8)]: +, sample 1; △, sample 2; ○, sample 3; +, sample 4; ▲, sample 5; ●, mixture 1; ▽, mixture 2.

Here the standard deviation is 0.013. It is clear that the Glicksman model is to be preferred here.

In the same way, our heat transfer measurements are presented in Figs. 4 and 5. In Fig. 4 the measured Nusselt numbers are presented, compared with the Nusselt numbers calculated with relation (2) with the use of equations (7) and (8). Calculated values seem to
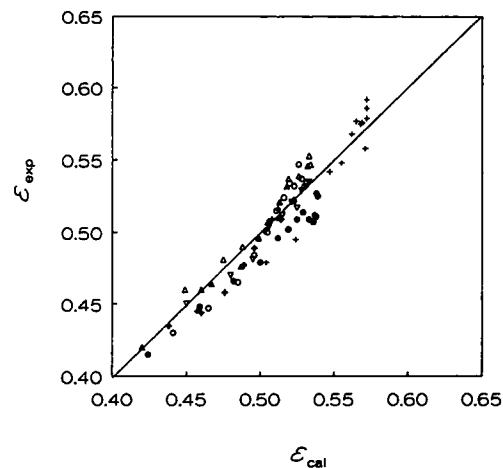

FIG. 3. Comparison between experimental results (samples 1–5 and mixtures 1, 2) and model calculations [equations (9)–(13)]: +, sample 1; △, sample 2; ○, sample 3; +, sample 4; ▲, sample 5; ●, mixture 1; ▽, mixture 2.
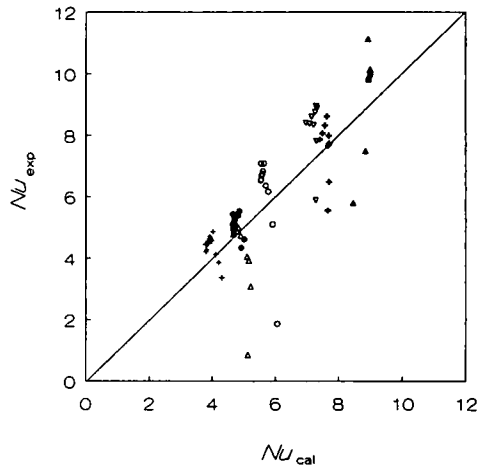
Fig. 4. Comparison between experimental results (samples 1–5 and mixtures 1, 2) and model calculations [equation (2), using equations (7) and (8)]: +, sample 1; △, sample 2; ○, sample 3; +, sample 4; ▲, sample 5; ●, mixture 1; ▽, mixture 2.

be almost constant: hardly any influence of fluidizing velocity on heat transfer is shown. The standard deviation is 1.19. In Fig. 5 measurements are shown, compared to equation (6) using (9)–(13). Measurements vary along the line $Nu_{cal} = Nu_{exp}$ which shows the influence of velocity. Here the standard deviation is 1.08.

Conclusions from these results are that the porosity model developed by Glicksman et al. [3] gives closer predictions than the porosity equations advised by Borodulya et al. [2] and that the use of this model, together with the modification for low velocities advised here, improves accuracy of the prediction of
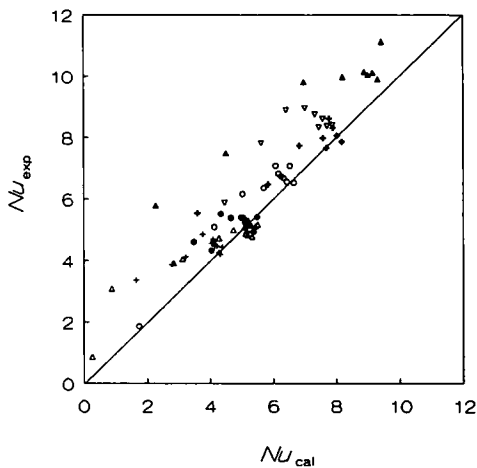

Fig. 5. Comparison between experimental results (samples 1–5 and mixtures 1, 2) and model calculations [equation (6), using equations (9)–(13)]: +, sample 1; △, sample 2; ○, sample 3; +, sample 4; ▲, sample 5; ●, mixture 1; ▽, mixture 2.

the heat transfer coefficient by Borodulya's model. The heat transfer coefficient of sand with a wide particle size distribution can also be calculated with the model, using equation (14). We emphasize that the fluidized bed we used in our experiments was of different magnitude than those used by Borodulya et al. [2] and Glicksman et al. [3] and recognize that deviation from our results is possible in different sized beds.

REFERENCES

1. V. A. Borodulya, Yu. S. Teplitsky, I. I. Markevich, A. F. Hassan and T. P. Yeryomenko, Heat transfer between a surface and a fluidized bed: consideration of pressure and temperature effects, Int. J. Heat Mass Transfer 34, 47–53 (1991).
2. V. A. Borodulya, V. L. Ganzha, Yu. S. Teplitsky and Yu. G. Epanov, Heat transfer in fluidized beds, J. Engng Phys. 49(4), 621–626 (1985).
3. L. R. Glicksman, T. Yule and A. Dyrness, Prediction of the expansion of fluidized beds containing tubes, Chem. Engng Sci. 46, 1561–1571 (1991).
4. A. I. Tamarin and Yu. S. Teplitsky, Expansion of an inhomogeneous fluidized bed, J. Engng Phys. 32(3), 469–473 (1977).

APPENDIX

Table A1. Porosity measurements

Velocity	Experimental value	Borodulya	Glicksman
Fraction 1			
0.155	0.445	0.463	0.457
0.273	0.479	0.503	0.504
0.364	0.495	0.527	0.524
0.449	0.509	0.544	0.537
0.537	0.542	0.560	0.547
0.635	0.548	0.575	0.555
0.757	0.568	0.590	0.562
0.848	0.577	0.600	0.565
0.945	0.575	0.611	0.568
1.035	0.576	0.619	0.569
1.135	0.558	0.628	0.571
1.238	0.579	0.636	0.572
1.349	0.586	0.644	0.572
1.488	0.592	0.653	0.572
Fraction 2			
0.243	0.420	0.421	0.420
0.352	0.460	0.450	0.449
0.446	0.481	0.489	0.475
0.523	0.490	0.509	0.488
0.647	0.507	0.534	0.505
0.742	0.510	0.549	0.513
0.839	0.537	0.563	0.519
0.933	0.523	0.576	0.523
1.028	0.539	0.586	0.526
1.129	0.532	0.597	0.529
1.235	0.546	0.607	0.532
1.346	0.553	0.617	0.533
1.430	0.547	0.624	0.534

Table A1.—*Continued*

Velocity	Experimental value	Borodulya	Glicksman
Fraction 3			
0.459	0.430	0.449	0.441
0.550	0.447	0.481	0.465
0.658	0.465	0.515	0.485
0.747	0.484	0.532	0.496
0.857	0.500	0.551	0.505
0.953	0.515	0.565	0.511
1.056	0.524	0.579	0.516
1.162	0.534	0.591	0.520
1.256	0.532	0.601	0.523
1.374	0.547	0.612	0.526
1.508	0.537	0.623	0.528
Fraction 4			
0.675	0.435	0.436	0.438
0.769	0.444	0.448	0.460
0.871	0.458	0.465	0.476
0.984	0.477	0.484	0.489
1.081	0.489	0.501	0.496
1.178	0.501	0.517	0.503
1.280	0.509	0.535	0.508
1.393	0.516	0.554	0.512
1.472	0.509	0.567	0.514
Fraction 5			
0.817	0.460	0.460	0.460
0.913	0.464	0.466	0.467
1.006	0.476	0.476	0.487
1.108	0.496	0.490	0.499
1.197	0.508	0.504	0.506
1.303	0.521	0.518	0.513
1.382	0.532	0.529	0.518
1.505	0.522	0.546	0.522
Mixture 1			
0.224	0.415	0.426	0.424
0.306	0.448	0.464	0.459
0.398	0.466	0.492	0.482
0.502	0.479	0.516	0.500
0.612	0.496	0.537	0.512
0.701	0.502	0.551	0.519
0.795	0.509	0.563	0.525
0.905	0.514	0.578	0.529
1.010	0.509	0.589	0.533
1.108	0.507	0.599	0.536
1.200	0.512	0.607	0.537
1.315	0.527	0.616	0.538
1.382	0.511	0.621	0.538
1.431	0.525	0.625	0.539
Mixture 2			
0.600	0.450	0.450	0.450
0.696	0.470	0.465	0.480
0.795	0.481	0.482	0.495
0.896	0.504	0.498	0.506
1.006	0.512	0.517	0.515
1.108	0.521	0.533	0.521
1.200	0.517	0.549	0.525
1.292	0.529	0.564	0.528
1.388	0.534	0.580	0.531
1.470	0.535	0.593	0.533

Table A2. Heat transfer measurements

Velocity	Experimental value	Borodulya	Glicksman
Fraction 1			
0.169	3.36	4.30	1.65
0.254	3.86	4.20	2.78
0.329	4.12	4.11	3.22
0.472	4.86	4.02	3.77
0.563	4.57	3.98	4.05
0.624	4.63	3.95	4.08
0.707	4.70	3.92	4.09
0.785	4.62	3.90	4.11
0.848	4.47	3.88	4.14
0.937	4.55	3.86	4.17
1.049	4.47	3.84	4.22
1.175	4.27	3.82	4.28
1.256	4.20	3.80	4.32
1.355	4.44	3.79	4.38
Fraction 2			
0.189	0.85	5.13	0.26
0.268	3.08	5.22	0.88
0.340	3.92	5.16	2.84
0.360	4.05	5.10	3.12
0.495	4.73	4.90	4.28
0.600	4.99	4.83	4.74
0.707	4.88	4.78	5.13
0.799	5.10	4.75	5.10
0.905	4.96	4.71	5.15
0.980	4.83	4.70	5.20
1.095	4.88	4.68	5.27
1.181	4.78	4.66	5.34
1.231	5.03	4.66	5.37
1.315	5.12	4.65	5.44
1.399	5.17	4.64	5.51
Fraction 3			
0.433	1.86	6.06	1.74
0.537	5.09	5.91	4.13
0.635	6.16	5.77	5.03
0.747	6.36	5.69	5.70
0.852	7.08	5.63	6.08
0.945	6.83	5.60	6.17
1.035	6.74	5.58	6.25
1.129	6.69	5.56	6.33
1.238	6.56	5.55	6.44
1.326	7.08	5.54	6.53
1.447	6.53	5.53	6.66
Fraction 4			
0.690	5.54	7.65	3.59
0.785	6.48	7.69	5.84
0.880	7.73	7.69	6.83
0.984	7.98	7.68	7.58
1.046	7.66	7.66	7.68
1.138	8.61	7.62	7.77
1.231	8.31	7.56	7.89
1.335	8.06	7.48	8.02
1.436	7.86	7.40	8.17
Fraction 5			
0.747	5.79	8.45	2.27
0.880	7.49	8.84	4.50
0.965	9.81	8.93	6.97
1.056	9.98	8.97	8.20
1.158	10.15	8.99	8.89
1.250	10.05	8.99	9.00
1.349	10.12	8.97	9.15
1.447	9.91	8.94	9.31
1.570	11.13	8.92	9.43

Table A2.—*Continued*

Velocity	Experimental value	Borodulya	Glicksman
Mixture 1			
0.350	4.61	5.01	3.48
0.433	4.33	4.92	4.04
0.509	5.52	4.86	4.34
0.594	5.39	4.82	4.66
0.727	5.40	4.76	4.99
0.813	5.40	4.74	5.05
0.909	5.24	4.71	5.11
1.002	5.30	4.70	5.17
1.115	5.14	4.68	5.25
1.191	5.15	4.67	5.27
1.292	4.94	4.66	5.39
1.404	5.42	4.65	5.49
Mixture 2			
0.647	5.88	7.27	4.46
0.737	7.81	7.29	5.62
0.839	8.88	7.30	6.41
0.941	8.95	7.28	7.01
1.035	8.75	7.25	7.32
1.149	8.33	7.20	7.45
1.244	8.60	7.14	7.57
1.343	8.37	7.07	7.71
1.460	8.40	6.96	7.88